J. Iron Steel Res. Int. (2021) 28:1180–1189
https://doi.org/10.1007/s42243-021-00644-9

ORIGINAL PAPER

Effect of sliding speed on elevated-temperature wear behavior of AISI H13 steel

Yin Zhou[1] · Wei Jiang[2]

Received: 13 February 2021 / Revised: 11 March 2021 / Accepted: 22 March 2021 / Published online: 5 August 2021

Abstract
Elevated-temperature wear tests were performed on AISI H13 steel under 50 and 100 r/min at 400–600 °C. Through examining the morphology, structure and composition of worn surfaces as well as the microhardness at subsurfaces, the wear mechanisms in various sliding conditions were explored. H13 steel exhibited totally different elevated-temperature wear behavior at two sliding speeds while the high sliding speed would seriously deteriorate its wear resistance. During sliding at two sliding speeds, the wear rate of H13 steel decreased first and then rose with the increase in temperature and the wear rate reached the lowest value (lower than 1×10^{-6} mm^3/mm) at 500 °C and 50 r/min. The wear rate at 600 °C was lower than that at 400 °C for 50 r/min, but the wear rate at 600 °C was higher than that at 400 °C for 100 r/min (except for 50 N). At 50 r/min, the wear rate decreased first and then increased with the increase in load. However, at 100 r/min, the wear rate monotonically increased with increasing load and reached 33×10^{-6} mm^3/mm at 600 °C and 150 N, where severe wear occurred. In the other sliding conditions, severe wear did not appear with wear rate lower than 5×10^{-6} mm^3/mm. Oxidative mild wear merely prevailed at 500 °C and 50 r/min and oxidative wear appeared in the other sliding conditions except for 600 °C and 150 N, where severe plastic extrusion wear prevailed. The effect of sliding speed on wear behavior was attributed to the changes of tribo-oxide layers. During elevated-temperature sliding, tribo-oxide particles were more readily retained to form protective tribo-oxide layers on worn surfaces at the lower sliding speed than at the higher sliding speed, so as to protect from wear.

Keywords AISI H13 steel · Dry sliding wear · Elevated-temperature wear · Wear testing · Surface analysis · Wear mechanism · Sliding speed

1 Introduction

Hot-working dies are widely used as an important processing tool in modern industry, which endure strong extrusion and continuous friction of elevated-temperature metals during working. In such harsh high-temperature and high-load working conditions, elevated-temperature wear is one of the important failure forms of hot-working dies [1–3]. As a popular hot-working die steel, AISI H13 steel is widely used to fabricate hot hammer, hot forging and hot extrusion dies, etc. [4–9]. The surface temperature of the die cavity is usually much higher than the ambient temperature because of the contacted elevated-temperature metal and the released friction heat. The service temperature of hot-working dies was reported to range from 400 to 600 °C [5]. During elevated-temperature sliding, tribo-oxides are well known to form on worn surfaces of steels readily. Such a ceramic-characteristic layer avoids the direct contact between metal alloys, thus changing the wear performance of sliding pairs, which is so-called oxidative-type wear [5, 6]. In the hot-working process, continuous mechanical and thermal loadings apply to dies, finally leading to a heavy damage of the die surface. Thereinto, the elevated-temperature wear was proved to be an important limiting factor for the service life of dies [1–6]. Therefore, how to control oxidative-type wear to elevate

✉ Yin Zhou
626819302@qq.com

[1] School of Shipping and Mechatronic Engineering, Taizhou University, Taizhou 225300, Jiangsu, China

[2] Light Alloy Research Institute, Central South University, Changsha 410083, Hunan, China

the wear resistance of steels is the key to prolong the life of hot-work dies.

Regarding the researches on oxidative-type wear, some oxidative wear models were proposed, in which the oxidative wear theories suggested by Quinn et al. [10, 11] and Wilson et al. [12] were popularly accepted. In the oxidative wear model of Quinn et al. [10, 11], an oxidative mild wear prevails at room and slightly elevated temperatures and a tribo-oxide layer is in situ produced and thickened on the asperities of the contacting area. As the tribo-oxide layer reaches a critical thickness, it is totally delaminated. This oxidative mild wear is a cyclical process containing the formation, thickening and delamination of the tribo-oxide layer. However, the model of Wilson et al. [12] applies to the mild wear conditions: elevated temperatures, low speed and low load. In their model, the wear oxide debris particles would form nano-structured glaze layers at a higher temperature to enhance wear resistance [12]. During sliding, the gathering, compaction and sintering of oxide debris on worn surfaces are considered to affect the formation process of the tribo-oxide layers, but their delamination is a gradual process, different from the model of Quinn et al. [10, 11]. It is clear that the above models are based on mild wear or mild sliding conditions. A lot of researches on the oxidative wear were performed, and the wear-reduced effect of tribo-oxides was confirmed [1–6]. However, as sliding condition became severe, the oxidative-type wear does not follow the models of Quinn et al. and Wilson et al. [13, 14]. In these cases, tribo-oxides are uncertain to reduce wear, which conversely would accelerate wear gradually. Recently, Wang et al. [15, 16] studied elevated-temperature wear of steels and noticed that oxidative mild wear could not be sustained as the load surpassed a certain value. They pointed out that in this case, an oxidative mild-to-severe wear transition would occur and proposed to classify oxidative-type wear into oxidative mild wear and oxidative wear [15, 16]. The former follows the model of Quinn et al. [10, 11] or Wilson et al. [12]. However, the latter actually falls in a mild-to-severe wear transition region of oxidative wear [15, 16]. At present, the wear failure mechanism of H13 steel at 400–600 °C is unclear. In particular, the study on the effect of sliding speed on elevated-temperature wear was rarely reported.

In the present research, elevated-temperature wear tests were performed on H13 steel at 400–600 °C and the elevated-temperature wear behavior under various sliding conditions was studied. The purpose of this study is to explore the elevated-temperature wear behavior and failure mechanism under different sliding speeds. The morphology, phase, composition and property of worn surfaces and subsurfaces were investigated by scanning electron microscopy (SEM), X-ray diffractometry (XRD), energy-dispersive spectrometry (EDS) and microhardness test. Finally, the wear mechanism in various sliding conditions was disclosed.

2 Experimental procedure

The sliding pins and counterface disks were made from AISI H13 and AISI M2 steels, respectively, and their compositions are summarized in Table 1. H13 steel was austenitized for 20 min at 1020 °C, then quenched in oil, and finally tempered at 600 °C for 2 h to attain tempered martensite with a hardness of 46–48 HRC. M2 steel was austenitized for 30 min at 1180 °C in a salt bath furnace and quenched in oil, and then tempered three times at 540 °C for 120 min to reach 62–64 HRC. The heat-treated H13 and M2 steels were cut using a wire-electrode cutting machine into the pins with the sizes of ϕ4.7 mm × 12.7 mm and the disks with the sizes of ϕ54 mm × 8 mm, respectively. Before wear tests, the sliding surfaces of pins and disks were polished by 1200 grit sandpaper to achieve the roughness of 0.45 and 0.40 μm, respectively.

Elevated-temperature wear tests were performed on an MMU-5GA-type high temperature wear tester with the following experimental parameters: the temperatures of 400, 500 and 600 °C, the loads of 50, 100 and 150 N, sliding speeds of 50 and 100 r/min (0.095 and 0.190 m/s, respectively) and sliding distance of 684 m. Each pin was cleaned with acetone in an ultrasonic cleaning machine before and after wear test. After cleaning, the pin was weighed by an analytical balance with an accuracy of 0.01 mg. Each wear test was repeated three times to achieve the average value of mass loss (ΔM). Finally, the wear rate (W) was calculated through $W = \Delta M/(\rho S)$, where ρ is the density of the steel and S is the sliding distance.

SEM (JSM-7001F), EDS (Inca Energy, 350EDS) and XRD (D/Max-2500/pc) were employed to examine the morphology, composition and phase of worn surfaces and their sections. The microhardness of the tribo-layer and the subsurface matrix was measured using a digital microhardness meter (HVS-1000 type) at a load of 0.5 N and retention time of 15 s. An HR-150A Rockwell hardness meter was used to measure the hardness of the heat-treated steels.

3 Results and analysis

3.1 Tribological behavior of H13 steel

Figure 1 illustrates the variation of the wear rate of H13 steel with a series of temperatures and loads at two sliding speeds. The wear rate of H13 steel decreased first and then

Table 1 Chemical compositions of H13 steel and M2 steel (mass%)

Steel	C	Si	Cr	Mn	V	Mo	S	P	Fe
H13	0.42	1.04	5.15	0.43	0.90	1.45	≤ 0.030	≤ 0.030	Balance
M2	0.87	0.35	4.20	0.29	1.98	5.01	≤ 0.030	≤ 0.030	Balance

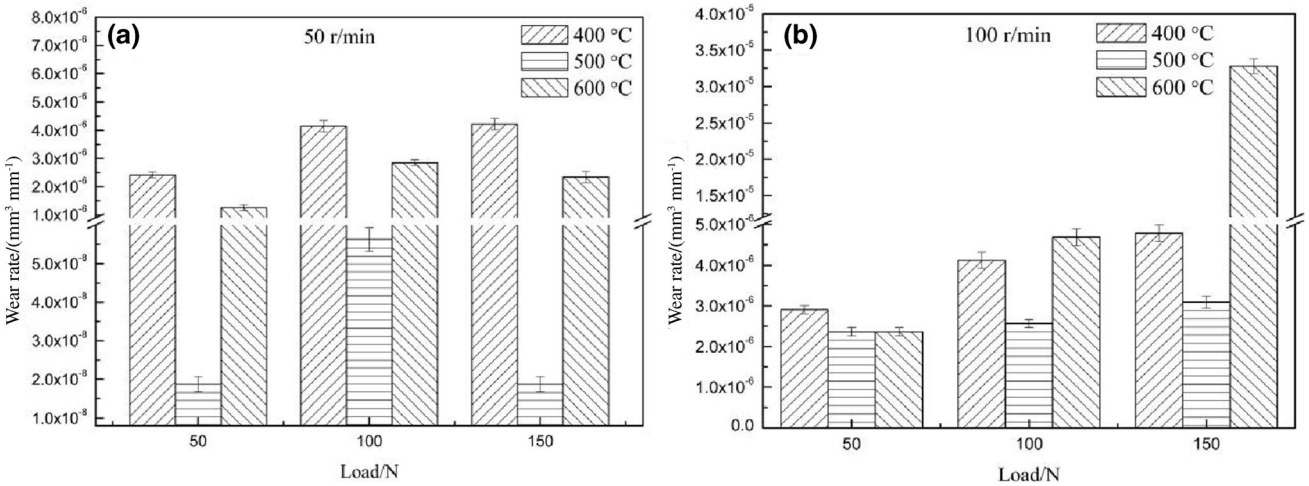

Fig. 1 Wear rate of H13 steel under two sliding speeds. **a** 50 r/min; **b** 100 r/min

increased with an increase in the temperature from 400 to 600 °C, regardless of sliding speed and load. The wear rate at 500 °C reached the lowest value, which was significantly lower than those at 400 and 600 °C (except for the case at 100 r/min and 50 N). Under 50 r/min, the wear rate was the lowest at 500 °C, the middle at 600 °C and the highest at 400 °C under each load. When the sliding speed increased to 100 r/min, the wear rate at 500 °C was still the lowest, but the variation of wear rate at 400 and 600 °C depended on load. Under the low load (50 N), the wear rate at 400 °C was slightly higher than that at 600 °C. With the increase in load, both the wear rates at 400 and 600 °C increased. However, the wear rate at 600 °C was higher than that at 400 °C and 100 N. Even at 150 N, the wear rate of 600 °C was more than 7 times that of 400 °C.

Under 50 r/min, the wear rate decreased first and then increased with the increase in load, while the wear rate increased monotonically at 100 r/min, and even reached 33×10^{-6} mm^3/mm at 600 °C and 150 N. It is clear that severe wear occurred under 100 r/min and 150 N at 600 °C. In other sliding conditions, the wear rates were lower than 5×10^{-6} mm^3/mm. As is described above, the wear behavior of H13 steel changed as a function of load, temperature and sliding speed. It was supposed that the variation of wear behavior could be attributed to the change of the wear mechanism of H13 steel.

Table 2 shows the average friction coefficients of H13 steel under various sliding conditions. At various temperatures except for the case of 600 °C, 100 r/min and 150 N, the friction coefficient decreased with the increase in the load. This is probably because large load produced more oxides as solid lubricant at high temperatures. It was noticed that the friction coefficient at 50 r/min was less than that at 100 r/min. Under the same load and temperature, the sliding surface at 100 r/min bore more shear force than that at 50 r/min. This meant that the sliding speed would change the state of sliding surfaces. Without considering the sliding speed and load, the friction coefficient presented a complex relationship with the temperature. Under 50 and 100 N, the friction coefficient decreased as the temperature rose from 400 to 500 °C, and then increased at 600 °C. However, under 150 N and 50 r/min, the friction coefficient monotonously increased with the increase in temperature. In the special case of 100 r/min and 600 °C, with the increase in load from 100 to 150 N, the friction coefficient did not drop but rose. This demonstrated that at 600 °C and 150 N, the higher sliding speed (100 r/min) caused worse sliding cases than the lower sliding speed (50 r/min).

3.2 Phases, macro- and micro-morphologies of worn surfaces

Figure 2 shows XRD patterns of worn surfaces at 150 N under different sliding conditions. At 400 °C and 100 r/min, no oxide peak was identified on worn surfaces,

Table 2 Average friction coefficient of H13 steel under different sliding conditions

Temperature/°C	Load/N	Friction coefficient	
		50 m min^{-1}	100 m min^{-1}
400	50	0.76	0.93
	100	0.50	0.51
	150	0.32	0.39
500	50	0.64	0.86
	100	0.43	0.59
	150	0.42	0.48
600	50	0.70	0.89
	100	0.54	0.62
	150	0.53	0.73

except α-Fe peaks. However, as the sliding speed dropped to 50 r/min at the same temperature, a small amount of Fe_2O_3 appeared on the worn surface. When the ambient temperature increased to 500 °C, the amount of oxides on the worn surface increased obviously which existed mainly in the form of Fe_3O_4 and Fe_2O_3. It was found that more oxides appeared at 50 r/min than at 100 r/min. This demonstrated that more oxides existed on worn surfaces at lower sliding speeds.

It was found that under the condition of 50 r/min, 150 N and 400 °C, a small amount of Fe_2O_3 and Fe_3O_4 appeared on the worn surface. As the ambient temperature rose to 500 °C, more Fe_2O_3 and Fe_3O_4 and a small amount of FeO were produced on worn surfaces. When the ambient temperature reached 600 °C, a great amount of oxides appeared, while α-Fe peaks became weaker. It is understandable that more oxides were produced at a higher temperature. However, it is questionable that the amount of oxides decreased at a higher speed (100 r/min).

Wear characteristics are readily identified from the macroscopic morphology of worn surfaces, especially their variations in size and color. Figure 3 shows the macroscopic morphology of worn surfaces of H13 steel at different temperatures and sliding speeds under 150 N. At 400 °C and 50 r/min (Fig. 3a), the worn surface presented a fine furrow parallel to the sliding direction and a blue luster of metal oxidation with yellowish red in the center. When the ambient temperature rose to 500 °C (Fig. 3b), the worn surface presented a reddish brown luster and undistinguished furrows. When the ambient temperature rose to 600 °C, a blue-gray gloss appeared on the whole surface (Fig. 3c). It looked as if a layer of enamel was attached to the worn surfaces with wide furrows and slightly extrusive deformation.

When the sliding speed increased to 100 r/min, the worn surface at 400 °C also presented fine furrows and a yellowish red luster, as shown in Fig. 3d. At 500 °C, the worn surface became dark red with fine furrows and slightly extrusive deformation (Fig. 3e). However, when the temperature rose to 600 °C (Fig. 3f), the worn surface presented a silver-gray metallic luster. More importantly, severe plastic deformation occurred throughout the worn surface with an appearance of the extrusive lip [14]. In this case, the sliding pin totally lost its original shape and size, and thus severe wear was considered to occur. It is clear that the color of metal oxidation was noticed on worn surfaces in most cases. However, at 600 °C, 150 N and 100 r/min, the color of metal oxidation disappeared and a metallic luster appeared instead. This demonstrated that oxidative-type wear finally turned into plastic-dominated wear with the increase in temperature, load and sliding

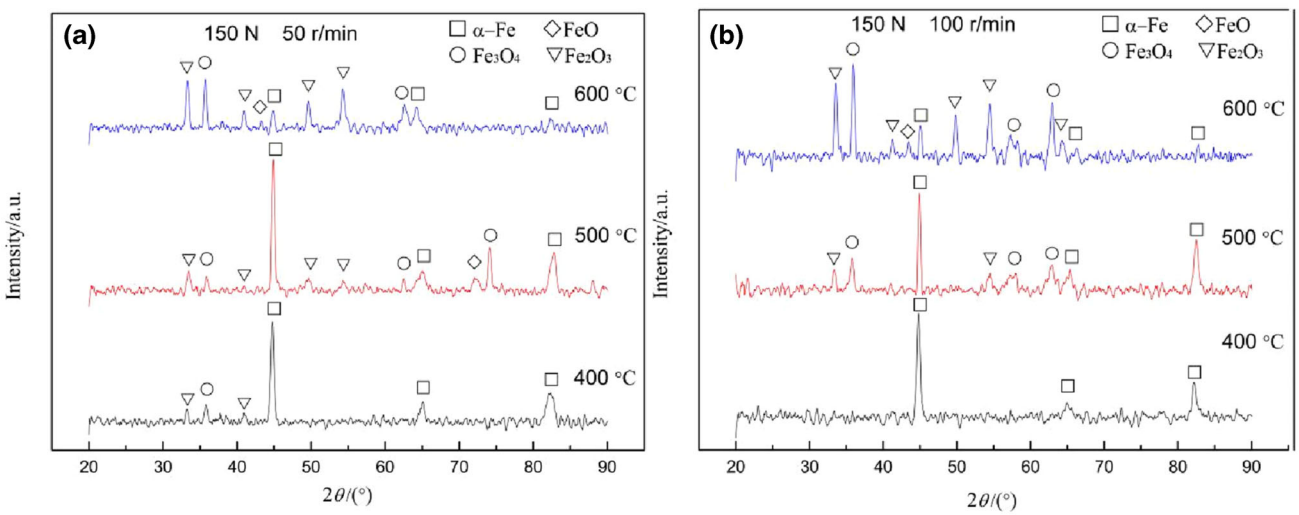

Fig. 2 XRD patterns of worn surfaces of H13 steel sliding at 50 r/min (**a**) and 100 r/min (**b**). 2θ Diffraction angle

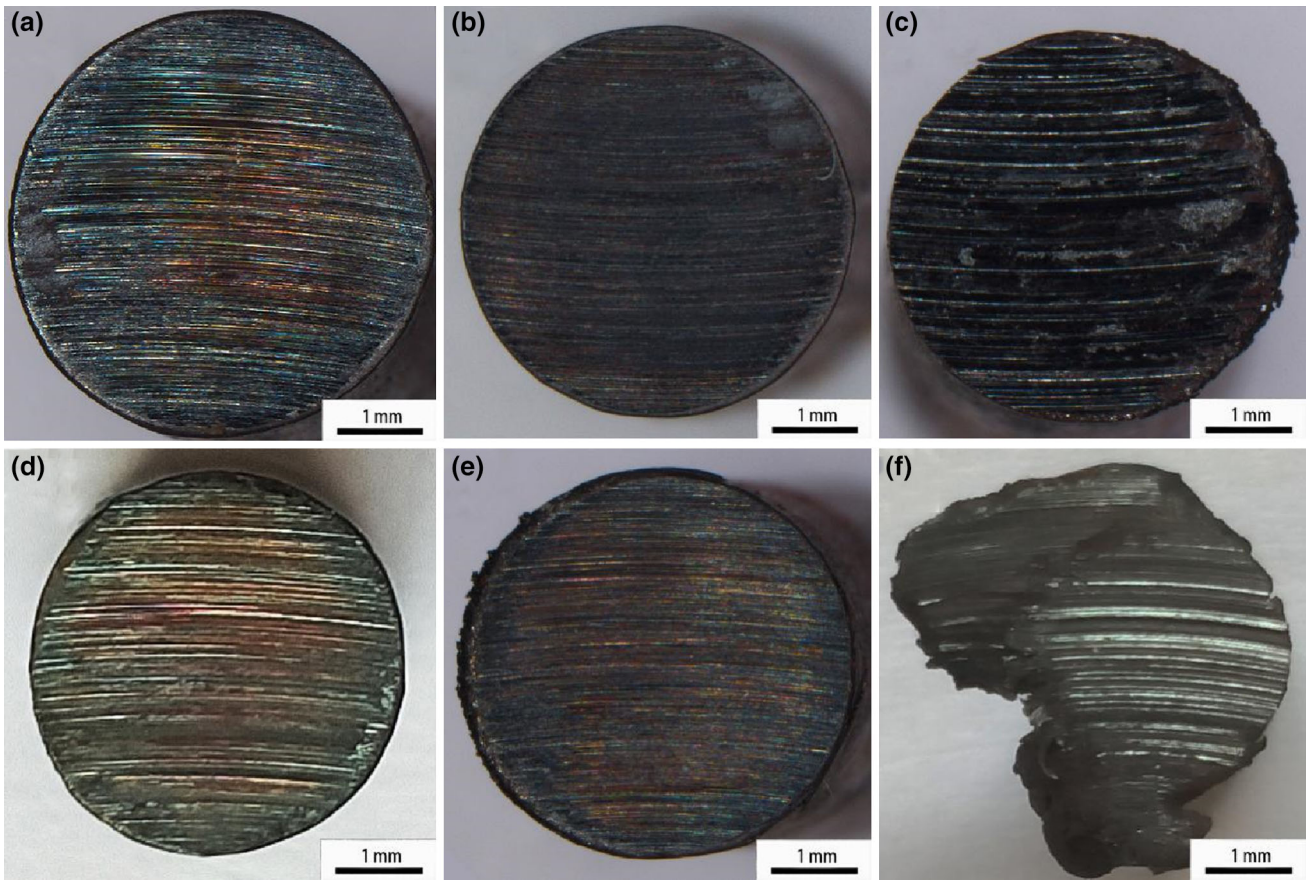

Fig. 3 Macroscopic morphology of worn surfaces of H13 steel sliding under 150 N at different temperatures and sliding speeds. **a** 400 °C, 50 r/min; **b** 500 °C, 50 r/min; **c** 600 °C, 50 r/min; **d** 400 °C, 100 r/min; **e** 500 °C, 100 r/min; **f** 600 °C, 100 r/min

speed. Hence, at the same high temperature and high load, the increase in sliding speed resulted in obvious variations of wear characteristics and wear mechanism.

SEM images of worn surfaces of H13 steel are shown in Fig. 4. At 400 °C, the worn surfaces presented obvious furrows at two sliding speeds, which would be produced by hard debris particles or the convex places of the counterface in the early stage of sliding. The debris particles on the worn surface were proved to be oxides by EDS analysis (Fig. 5a). It was also noticed that oxide particles at 100 r/min were less than those at 50 r/min. This indicated that as the sliding speed increased, oxide particles were not readily remained on worn surfaces. EDS analysis confirmed that less oxides existed on the worn surface at 100 r/min (Fig. 5b). At 500 °C, the worn surface presented smooth regions and rough ones, which corresponded to the tribo-layer and its peeling, respectively. Oxide particles would be readily identified to flock together in the rough region. The smooth regions were produced by aggregated oxide and metal particles under the action of high temperature and load. These are compiled with typical characteristics of oxidative wear [15, 16]. It was also seen that the spalling regions of the worn surface under 100 r/min seemed to be larger than those under 50 r/min. This meant that the higher speed caused more spalling of tribo-layers. At 600 °C and 50 r/min, the worn surface was mainly covered by smooth tribo-oxide layers with a small amount of spalling pits. When a load of 150 N at 100 r/min was applied, there appeared cracks perpendicular to the sliding direction. Hence, serious peeling would be expected during the continuous sliding.

3.3 Section morphology and hardness distribution at worn subsurfaces

Figure 6 illustrates the section morphology of worn surfaces of H13 steel sliding under 150 N. From the section morphology of worn surfaces, tribo-layers could be readily distinguished to be different from the matrix. Smooth, continuous or discontinuous tribo-layers were present on the worn surface, compared with the rough microstructure-showing matrix. More importantly, the tribo-layers possessed higher oxygen content, so-called tribo-oxide layers. In fact, they are mechanically mixed layers containing metal particles of the friction pair and their oxide particles [17]. At 400 °C and 50 r/min, the tribo-oxide layer was

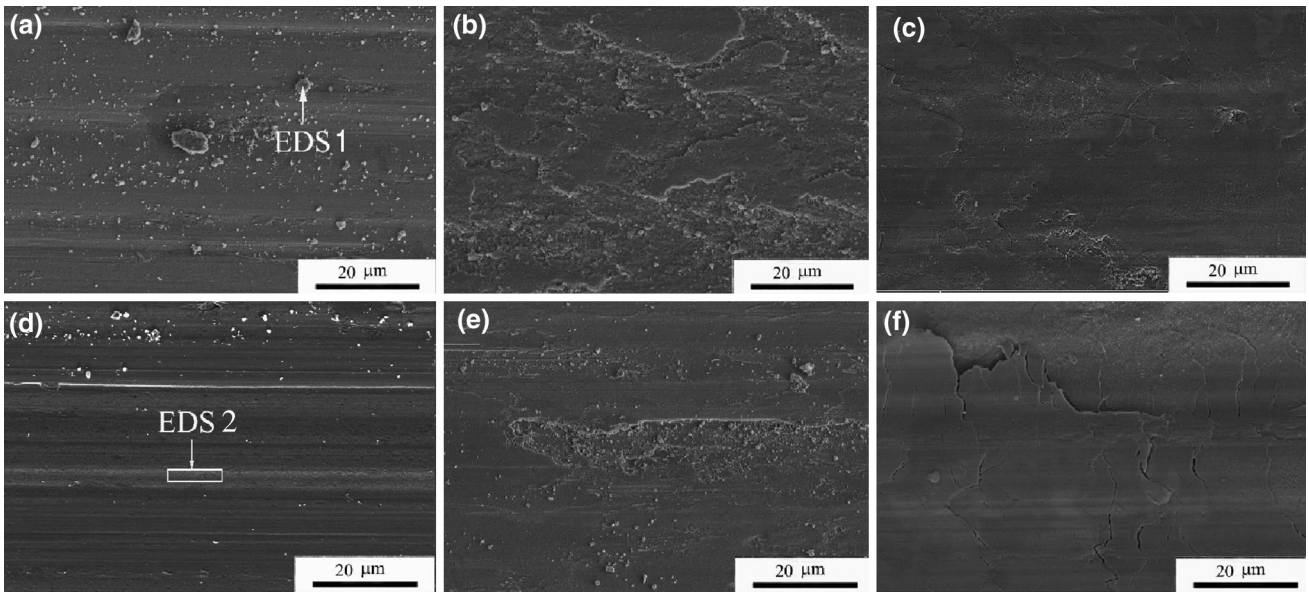

Fig. 4 SEM images of worn surfaces of H13 steel sliding under 150 N at different temperatures and speeds. **a** 400 °C, 50 r/min; **b** 500 °C, 50 r/min; **c** 600 °C, 50 r/min; **d** 400 °C, 100 r/min; **e** 500 °C, 100 r/min; **f** 600 °C, 100 r/min

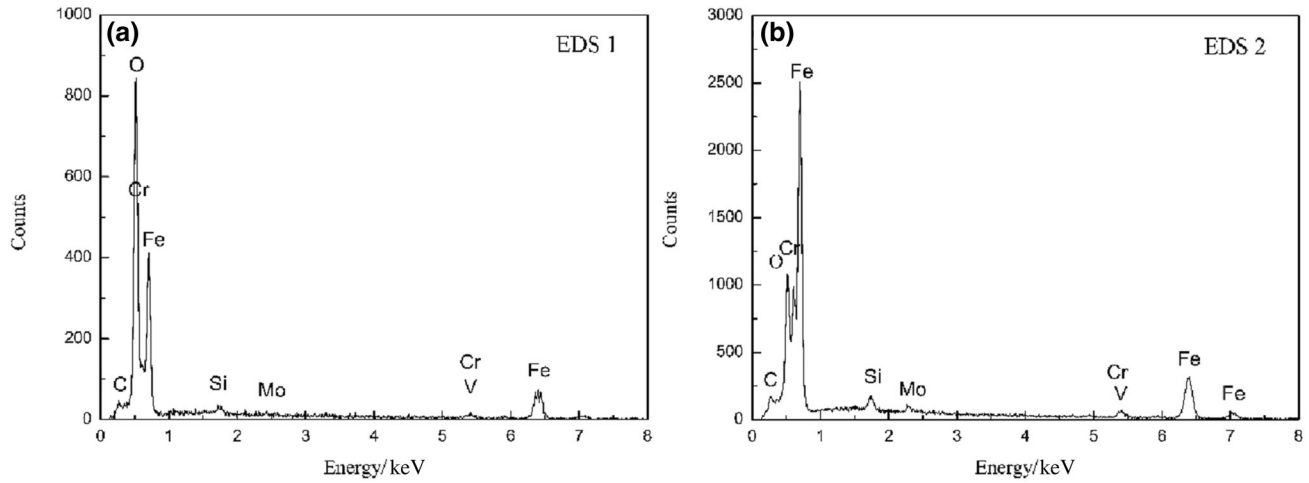

Fig. 5 EDS analysis of areas EDS 1 (**a**) and EDS 2 (**b**) marked in Fig. 4

discontinuous and about 5–10 μm in thickness (Fig. 6a). At 500 °C, the tribo-oxide layer became continuous and about 5–10 μm in thickness (Fig. 6b). When the ambient temperature reached 600 °C, the tribo-oxide layer thickened to about 10–30 μm; meanwhile, the subsurface matrix presented obvious plastic deformation traces (Fig. 6c). When the sliding speed increased to 100 r/min, the tribo-oxide layer became thinner with only 5 μm in thickness and discontinuous at 400 °C (Fig. 6d). At 500 °C, the tribo-oxide layer slightly thickened and became discontinuous (Fig. 6e). When the ambient temperature reached 600 °C, the tribo-oxide layer seemed to be broken and the cracks appeared, as shown in Fig. 6f. Comparing the morphology of tribo-oxide layers under two sliding speeds, it was noticed that the tribo-oxide layers at 50 r/min were more continuous, denser and thicker than those at 100 r/min. It was supposed that different wear behavior at two sliding speeds was attributed to the states of tribo-layers.

Figure 7 shows the microhardness distribution of the worn subsurfaces of H13 steel under 150 N. From the microhardness distribution of the worn subsurfaces, the property variation of the steel after wear would be evaluated. It was found that regardless of 50 or 100 r/min, the hardness of the worn subsurface gradiently decreased with

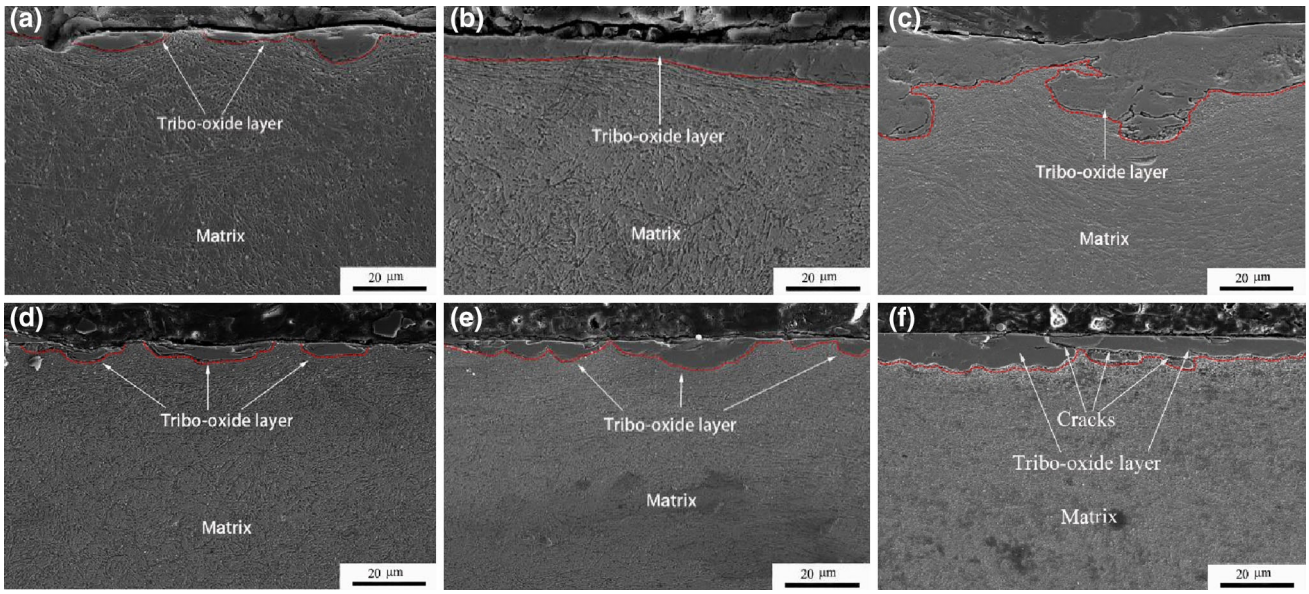

Fig. 6 Section morphology of worn surfaces of H13 steel under 150 N at different temperatures and sliding speeds. **a** 400 °C, 50 r/min; **b** 500 °C, 50 r/min; **c** 600 °C, 50 r/min; **d** 400 °C, 100 r/min; **e** 500 °C, 100 r/min; **f** 600 °C, 100 r/min

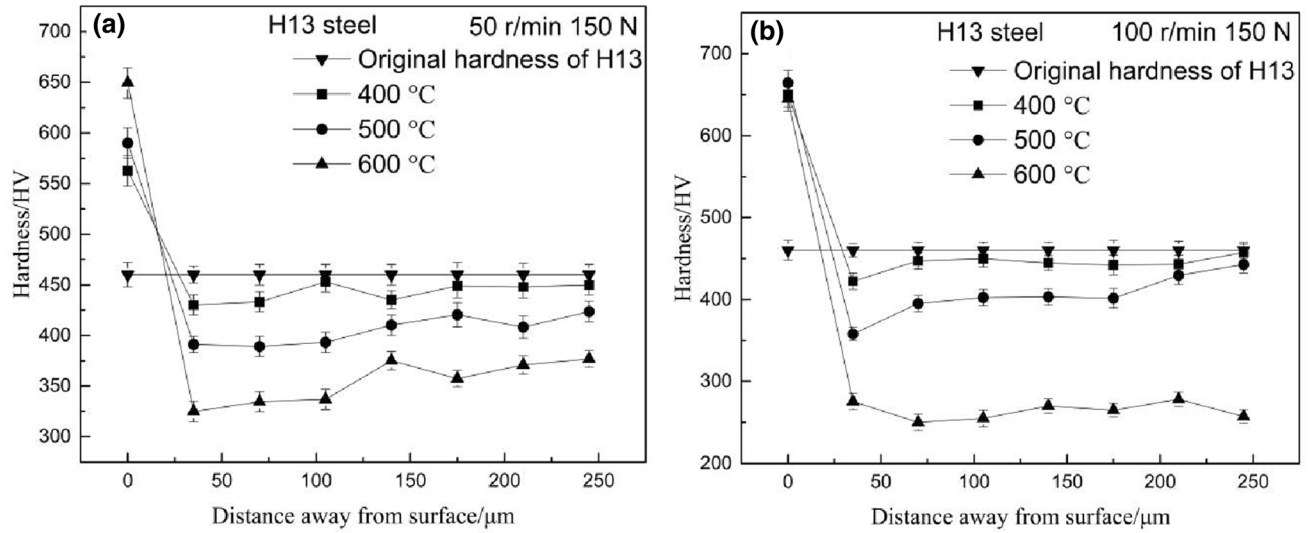

Fig. 7 Microhardness distribution of worn section subsurfaces of H13 steel at 150 N and different sliding speeds. **a** 50 r/min; **b** 100 r/min

increasing the distance from the worn surface. At 50 r/min (Fig. 7a), the outermost hardness reached 560–650 HV, and was significantly higher than that of the matrix. The outermost hardness could be roughly considered to be the hardness of the tribo-oxide layer. It was noticed that there was a 30-μm distance from the worn surface with the outermost hardness to the matrix. Moreover, the hardness of the matrix after wear was 440–450 HV at 400 °C, which was slightly lower than that (463 HV) of the original sample. This might be because the high friction heat and ambient temperature resulted in further tempering of subsurface matrix. As the ambient temperature increased to 500 and 600 °C, the hardness of the matrix at the subsurface markedly decreased to about 395–410 and 320–385 HV, respectively.

When the sliding speed was 100 r/min (Fig. 7b), the outermost hardness of the worn subsurface reached about 650 HV. The hardness decreased to be close to the matrix at 30 μm away from the worn surface. With the increase in ambient temperature, the matrix hardness decreased gradually from about 420–440 HV at 400 °C to 350–410 HV at 500 °C and 250–280 HV at 600 °C. Regardless of sliding speed, the matrix hardness of H13 steel was slightly reduced comparing with the original one at 400 and 500 °C. However, at 600 °C, the matrix hardness was substantially reduced, and especially the matrix hardness at

100 r/min was significantly lower than that at 50 r/min. The high sliding speed brought more friction heat and substantial increase in the contact temperature of the worn surface, so that the matrix hardness decreased more obviously to be less than 300 HV.

4 Discussion

4.1 Evaluation for wear resistance of H13 steel

In order to achieve higher service life of dies, mild wear is expected for the die steel during working. Nevertheless, mild and severe wear is a relative concept. How to maintain mild wear is a key problem for the application of hot-working dies. The severity of wear can be assessed from worn-surface roughness, wear debris size and wear rate. Usually, the wear rate is used to quantitatively divide mild wear and severe wear. In the research of So et al. [18], 1×10^{-6} mm^3/mm was proposed as the boundary line of oxidative mild wear. However, Zhang and Alpas [19] suggested 5×10^{-6} mm^3/mm as the boundary line of mild wear. However, Wang et al. [20] considered that mild wear and severe wear could not be divided by a line, but by a transition zone. In the present research, we took the suggestion of Wang et al. [20] to classify mild and severe wear. Based on the above-mentioned classifications, a transition region from 1×10^{-6} to 5×10^{-6} mm^3/mm was taken to divide mild and severe wear, in which the former was less than or equal to 1×10^{-6} mm^3/mm and the latter was more than 5×10^{-6} mm^3/mm.

As shown in Fig. 1, the wear rates of H13 steel under 50 r/min, 500 °C and 50–150 N were lower than 1×10^{-6} mm^3/mm, and mild wear prevailed. However, the wear rates of H13 steel under 50 r/min, 400 and 600 °C and 50–150 N as well as under 100 r/min, 400–600 °C and 50–150 N were greater than 1×10^{-6} mm^3/mm, but lower than 5×10^{-6} mm^3/mm (except for 600 °C and 150 N). Thus, in most cases, H13 steel did not fall in severe wear, but entered the mild-to-severe transition region. Nevertheless, when 150 N at 600 °C and 100 r/min was applied, the wear rate abruptly increased to 33×10^{-6} mm^3/mm and severe wear occurred. Impressively, in this case, the original shape and size of the pin were totally lost because of massively plastic deformation. This demonstrated that the sliding speed had a significant effect on the elevated-temperature wear behavior of H13 steel. With the increase in sliding speed from 50 to 100 r/min, the wear rate was noticed to increase substantially at various temperatures and loads, especially at 600 °C and 150 N. This meant that a high sliding speed would deteriorate the elevated-temperature wear resistance of H13 steel. All in all, in most cases of 400–600 °C, 50–100 r/min and 50–150 N, H13 steel fell in mild wear or the mild-to-severe wear transition region, presenting excellent wear resistance. Only at 100 r/min, 600 °C and 150 N, H13 steel fell in severe wear, presenting poor wear resistance.

The above analysis demonstrates that the wear severity of the steel presented some relations with the sliding speed. Thus, for the wear failure of hot-working dies, we must pay attention to the influence of the sliding speed or the loading speed of forging equipment. During working, the surfaces of the hot-working dies would occasionally reach 600 °C or above, and the local load would reach 150 N or more. It could be inferred that whether severe wear occurs or not, would depend on the sliding speed. When the sliding speed was 50 r/min (0.095 m/s) or below, such as hot extrusion dies, H13 steel could endure 400–600 °C and 50–150 N. However, as the sliding speed was 100 r/min (0.19 m/s) or above, such as hot forging dies, H13 steel could not endure the working conditions at 600 °C and 150 N and failed immediately.

4.2 Wear failure mechanism of H13 steel

During sliding of metal alloys, tribo-oxides are inevitably produced on the worn surface, especially at high temperature. Undoubtedly, the appearance of tribo-oxides changes the wear behavior and even wear mechanism for a given sliding pair. As shown in Fig. 2, tribo-oxides could be identified on worn surfaces in most cases at 400–600 °C and 50–150 N. Jiang et al. [21] pointed out that even though tribo-oxides could not be identified by XRD because of their trace amount, their real existence would affect the wear behavior and mechanism. Thus, even if no oxide was identified at 400 °C and 100 r/min, trace tribo-oxides would actually form on worn surfaces, as noticed from the oxidation color of worn surfaces in Fig. 3. As shown in Fig. 4a–e, typical oxidative wear characteristics were found, as reported in the studies [15, 16]. Undoubtedly, in most cases at 400–600 °C, oxidative-type wear prevailed. The only exception was the case under 600 °C, 100 r/min and 150 N and the metal luster was presented with massively plastic deformation on the worn surface. It is clear that a plastic-dominated wear prevailed in this case.

For oxidative-type wear, oxidation wear models proposed by Quinn et al. [10, 11] or Wilson et al. [12] belong to mild wear. It is clear that the wear of H13 steel under 50 r/min, 500 °C and 50–150 N fell in mild wear. The oxidation wear model proposed by Wilson et al. [12] seemed to apply to our current study. Wilson et al. [12] proposed the oxidation wear model for high temperature, low speed and low load. In their theory, wear debris particles are totally or partly oxidized to produce oxide particles or the mixture of oxides and metals during sliding, and are gradually compacted and sintered on worn surfaces under

the action of load at high temperature, finally forming a tight tribo-oxide layer. Ideally, this tribo-oxide layer is produced like enamel with complete and dense structure, avoiding the metal–metal contact, and thus protecting the sliding surface from further wear.

However, as the sliding condition intensifies further, the wear is beyond mild wear in spite of the existence of the oxidative characteristics of worn surfaces. Thus, the oxidation wear models proposed by Quinn et al. [10, 11] and Wilson et al. [12] are not applied in these cases. In recent researches, Wang et al. [15, 16] classified oxidative-type wear into oxidative mild wear and oxidative wear. The former followed the oxidation wear model proposed by Quinn et al. [10, 11] or Wilson et al. [12], but the latter did not, and fell in the mild-to-severe transition region.

Generally, the tribo-oxide layer was reported to be a mechanical mixing compounds including oxides and metals [17]. It usually presents discontinuous and uncompacted structures containing pores and cracks in severe sliding conditions. As sliding goes on, the tribo-oxide layer would be gradually consumed by peeling under the action of friction force. When the delamination and formation of tribo-oxide layers reached a dynamic equilibrium, mild wear prevailed. However, when the delamination of tribo-oxide layers was larger than their formation, their protection would be partly or totally lost, and the wear entered the mild-to-severe wear transition region or fell in severe wear.

Based on oxidation wear theory of Wilson et al. [12], metal wear debris is a prerequisite for the formation of tribo-oxide layers. During sliding, oxide particles form and aggregate on the worn surface due to high temperature environment and friction heat. The low sliding speed (50 r/min) made the oxide particles readily gather on the worn surface, and thus continuous and dense tribo-oxide layers would be formed under the combined action of force and high temperature. As the sliding speed increased to 100 r/min, most of the wear debris particles would be thrown out from worn surfaces and less ones remained to form discontinuous and thin tribo-oxide layers. Clearly, the continuous and dense tribo-oxide layers possessed more protective function than the discontinuous and thin ones. If cracks existed in tribo-oxide layers, their protective function would be greatly damaged.

From the morphology of tribo-oxide layers and wear rate, as shown in Fig. 6 and Fig. 1, their protective function and wear regime could be roughly achieved. At 50 r/min, 500 °C and 50–150 N, the tribo-oxide layers were considered to possess a totally protective function, so that mild wear prevailed. At 50 r/min, 400 and 600 °C and 50–150 N, as well as at 100 r/min, 400–600 °C and 50–150 N (except for 100 r/min, 600 °C and 150 N), the tribo-oxide layers only possess a partly protective function, and thus fell in the mild-to-severe wear transition region. Nevertheless, as 150 N were applied at 100 r/min and 600 °C, tribo-oxide layer fractured to totally lose its protection. In this case, under such a high temperature and load, because of lacking of the protection from tribo-oxide layers, massively plastic deformation occurred at the subsurface matrix, so that plastically extrusive wear prevailed, as reported by So et al. [14]. It was found that plastic flow occurred when the hardness of the matrix was below 300 HV at 100 r/min, 600 °C and 150 N. In this case, cracks and double layer morphology were noticed in the tribo-oxide layer. It was supposed that such a tribo-oxide layer presented no protection and plastic extrusion wear occurred because of the softened matrix. This demonstrated that wear mechanism depended not only on tribo-oxide layers, but also on the subsurface matrix [15, 16]. The relationship of wear mechanism with tribo-oxide layers, subsurface matrix hardness and sliding conditions is roughly summarized, as shown in Fig. 8.

On the basis of the above analysis for worn surfaces and wear severity, wear mechanisms under 400–600 °C and 50–150 N at 50 and 100 r/min were suggested as follows: oxidative mild wear prevailed under 500 °C and 50–150 N at 50 r/min; oxidative wear prevailed under 400–600 °C and 50–150 N at 50 r/min and 400–600 °C and 50–150 N at 100 r/min (except 600 °C and 150 N), and plastically extrusive wear prevailed under 600 °C and 150 N at 100 r/min.

5 Conclusions

1. H13 steel exhibits different elevated-temperature wear behavior as a function of load under two sliding speeds. At 50 r/min, the wear rate decreased first and then increased with increasing load. However, at 100 r/min, the wear rate monotonically increased with increasing load and reached 33×10^{-6} mm^3/mm at 600 °C and 150 N.
2. During sliding at two sliding speeds, the wear rate of H13 steel decreased first and then rose with increasing temperature. The wear rate reached the lowest value with lower than 1×10^{-6} mm^3/mm at 500 °C and that was lower at 600 °C than at 400 °C for 50 r/min, but the converse trend was presented for 100 r/min (except for 50 N).
3. Oxidative mild wear merely prevailed at 500 °C and 50 r/min and the wear entered the mild-to-severe wear transition region of oxidative wear in the other sliding conditions except at 600 °C and 150 N, where severe plastically extrusive wear prevailed. The oxidative mild wear complied with the oxidation wear model suggested by Wilson et al.

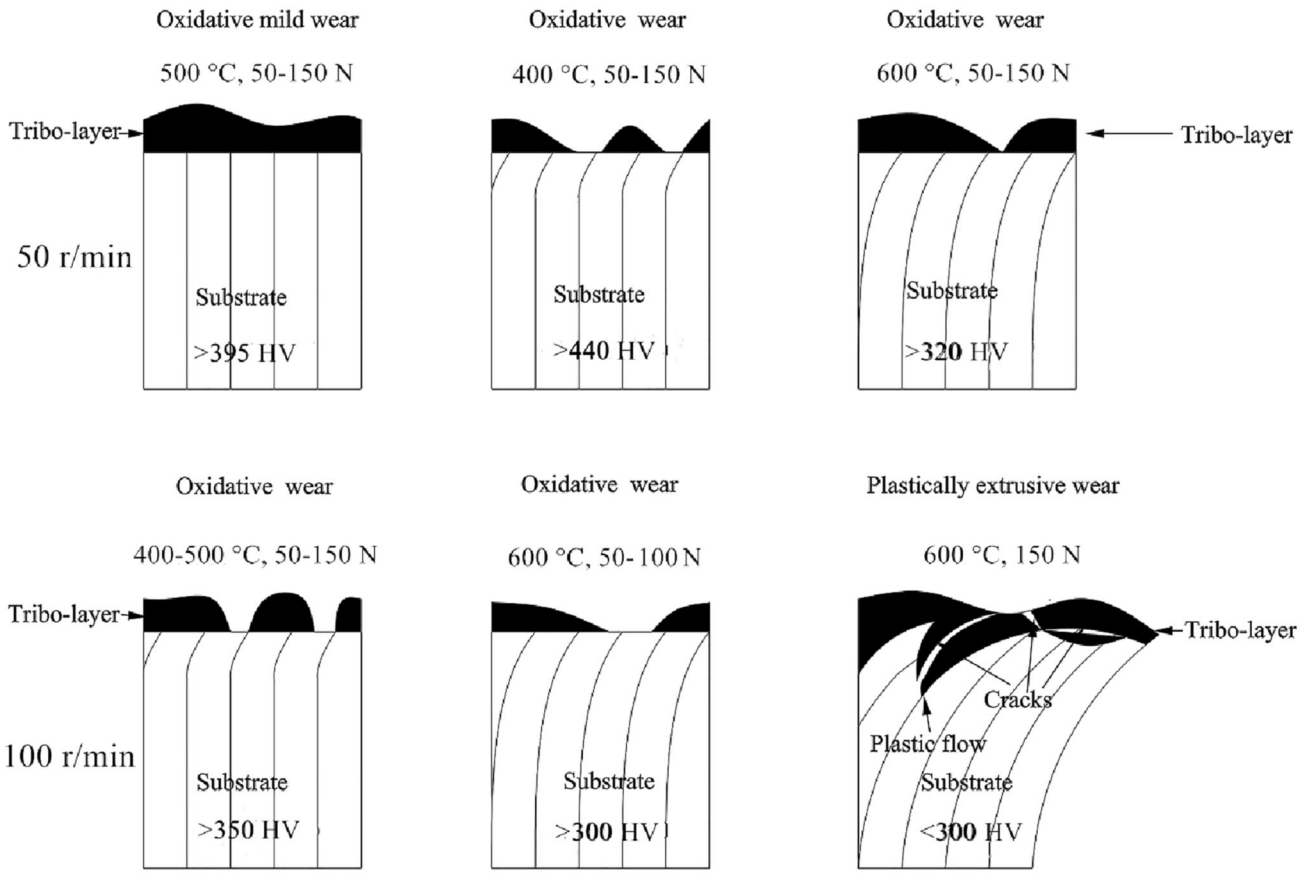

Fig. 8 Relationship of wear mechanism with tribo-oxide layers, subsurface matrix hardness and sliding conditions

4. In oxidative wear regime, sliding speed was noticed to affect the formation of tribo-oxide layers during sliding at high temperatures. At the lower sliding speed, tribo-oxide particles were readily retained on worn surfaces to form continuous and dense tribo-oxide layers so as to protect from wear. However, at higher sliding speed, when thermal softening of the subsurface matrix occurred at 600 °C and 150 N, the discontinuous and loose tribo-oxide layer lost its protective function.

Acknowledgements The authors are grateful for the financial support by Natural Science Foundation of Jiangsu Province (No. BK20201231), Jiangsu Colleges and Universities "Cyanine Engineering" and Research Startup Fund Project for High-level Talents of Taizhou University (No. TZXY2017QDJJ013).

References

[1] S. Li, X.C. Wu, S.H. Chen, J.W. Li, J. Mater. Eng. Perform. 25 (2016) 2993–3006.
[2] O. Barrau, C. Boher, R. Gras, F. Rezai-Aria, Wear 255 (2003) 1444–1454.
[3] S. Li, X.C. Wu, X.X. Li, J.W. Li, X.J. He, Tribol. Lett. 64 (2016) 32.
[4] X.H. Cui, S.Q. Wang, M.X. Wei, Z.R. Yang, J. Mater. Eng. Perform. 20 (2011) 1055–1062.
[5] H.P. Hua, Y. Zhou, X.X. Li, Q.Y. Zhang, X.H. Cui, S.Q. Wang, Proc. IMechE Part J J. Eng. Tribol. 229 (2015) 763–770.
[6] M.X. Wei, F. Wang, S.Q. Wang, X.H. Cui, Mater. Des. 30 (2009) 3608–3614.
[7] S.Y. Li, B. Li, X.M. Zhao, X.J. Xi, S.C. Duan, J. Guo, H.J. Guo, J. Iron Steel Res. Int. (2021). https://doi.org/10.1007/s42243-020-00532-8.
[8] C.M. Li, Y.B. Tan, F. Zhao, J. Iron Steel Res. Int. 27 (2020) 1073–1086.
[9] H.S. Chen, Y.Q. Wang, W.Q. Du, W. Liang, Y.X. Luo, J. Iron Steel Res. Int. 25 (2018) 580–588.
[10] J.L. Sullivan, T.F.J. Quinn, D.M. Rowson, Tribol. Int. 13 (1980) 153–158.
[11] T.F.J. Quinn, Wear 216 (1998) 262–275.
[12] J.E. Wilson, F.H. Stott, G.C. Wood, Proc. R Soc. Lond. A 369 (1980) 557–574.
[13] E. Marui, N. Hasegawa, H. Endo, K. Tanaka, T. Hattori, Wear 205 (1997) 186–199.
[14] H. So, H.M. Chen, L.W. Chen, Wear 265 (2008) 1142–1148.
[15] Q.Y. Zhang, K.M. Chen, L. Wang, X.H. Cui, S.Q. Wang, Tribol. Int. 61 (2013) 214–223.
[16] S.Q. Wang, L. Wang, Y.T. Zhao, Y. Sun, Z.R. Yang, Wear 306 (2013) 311–320.
[17] A. Pauschitz, M. Roy, F. Franek, Tribol. Int. 41(2008) 584–602.
[18] H. So, D.S. Yu, C.Y. Chuang, Wear 253 (2002) 1004–1015.
[19] J. Zhang, A.T. Alpas, Acta Mater. 45 (1997) 513–528.
[20] Y. Wang, T.Q. Lei, J.J. Liu, Wear 231 (1999) 1–11.
[21] W. Jiang, L. Wang, S.Q. Wang, Metall. Mater. Trans. B 51 (2020) 1127–1136.